Numerical simulation of inclined piles in liquefiable soils

Y Wang & R P Orense
Department of Civil and Environmental Engineering, University of Auckland, NZ.
ywan833@aucklanduni.ac.nz (Corresponding author)

Keywords: inclined pile; liquefaction; OpenSees; soil-pile interaction

ABSTRACT

A three-dimensional finite element model (3D FEM) has been developed in OpenSees to investigate the seismic response of inclined piles in liquefiable sand. The spring interface method is compared with the no interface approach in which pile and soil are bonded directly together to shed light on the effects of soil-pile interaction. By employing a Pressure-Dependent Multi-Yield surface material (PDMY02) model for the saturated sand, the seismic behaviour of sand under liquefaction is taken into consideration. By verifying modelled results with corresponding case studies on vertical pile in liquefied ground, the proposed modelling method is shown to be suitable for the simulation with acceptable accuracy. Based on the proposed model with inclined piles, a series of numerical analyses is conducted to examine the influence of raked angle and liquefaction on the seismic response of the model. It is concluded that pile inclination could be beneficial in reducing the lateral displacement of the superstructure but results in increasing pile shear forces. It is recommended that inclined piles are designed to accommodate these additional shear demands.

1 INTRODUCTION

Inclined piles are believed to be able to resist higher lateral loadings than vertical piles by transferring part of the lateral force into the axial direction. On one hand, evidences have revealed that the inclined piles designed properly may be beneficial for both the superstructure and piles themselves. For example, Berrill et al. (2001) investigated the Landing bridge in New Zealand after the 1987 Edgecumbe earthquake and found the effective impact of raked piles against lateral spreading. On the other hand, there are several frequently mentioned drawbacks resulting in the discouragement of the use of inclined piles in the seismic design of foundations. These drawbacks include residual bending moment due to soil consolidation (pre-earthquake) and settlement (post-earthquake), large kinematic force at the pile-cap connection, reduction in bending capacity due to the tensile axial forces and undesirable rotation on the cap supported by non-symmetrical batter piles (Gerolymos et al., 2008).

The beneficial or detrimental role of inclined piles on the dynamic behaviour of the superstructure and foundation is still not well established, despite numerous research carried out by means of laboratory tests and numerical investigations. Most of the laboratory experiments have been performed on dry sand or clay (Li et al., 2016; Subramanian & Boominathan, 2016). Only a few experiments focused on the seismic response of inclined piles in liquefiable soil (Dash & Bhattacharya, 2015; McManus et al., 2005). Numerical methods found in literature are mainly based on FEM methodology with different implementations, including sophisticated FEM models, coupled boundary element and FEM models and simplified non-linear system of springs and dashpots based on Winkler's assumptions. However, in most of the numerical simulations, the soil is modelled as elastic material for simplication (Ghorbani et al., 2014; Goit & Saitoh, 2013).

This paper discusses a series of 3D FEM analyses which were carried out through the platform of OpenSees (Open System for Earthquake Engineering Simulation), a freely available software

sponsored by PEER (Mazzoni et al., 2007). The seismic behaviour of liquefiable soil was taken into consideration by an appropriate constitutive soil model. A nonlinear spring soil-pile interface was adopted and compared with the no interface method in which the pile nodes were directly tied with the soil nodes. The numerical model was firstly verified by modelling a vertical pile and compared with experimental data. The model was then adopted for modelling inclined piles. By changing the raked angle of the pile (0°-20°), a parametric analysis was finally conducted to investigate the seismic response of the system.

2 VERTICAL SINGLE PILE ANALYSIS

2.1 Model description

In order to verify the numerical method, a vertical single pile was modelled and the results were compared with a centrifuge experiment (CSP3-J) from Wilson (1998). The prototype partial model layout is shown in Figure 1a. In the test, an aluminum pipe with an outer diameter of 670 mm and wall thickness of 19 mm was installed into the layered Nevada sand. The pile toe was about 3.9 m above the base and the pile head was about 3.8 m above the ground surface. The relative densities of the soil in liquefiable and non-liquefiable layers were about 55% and 80%, respectively. A superstructure weighing 49.1 ton was put on the pile head and the 1995 Kobe earthquake acceleration record (Figure 1b) was scaled to 0.22 g as the input motion.

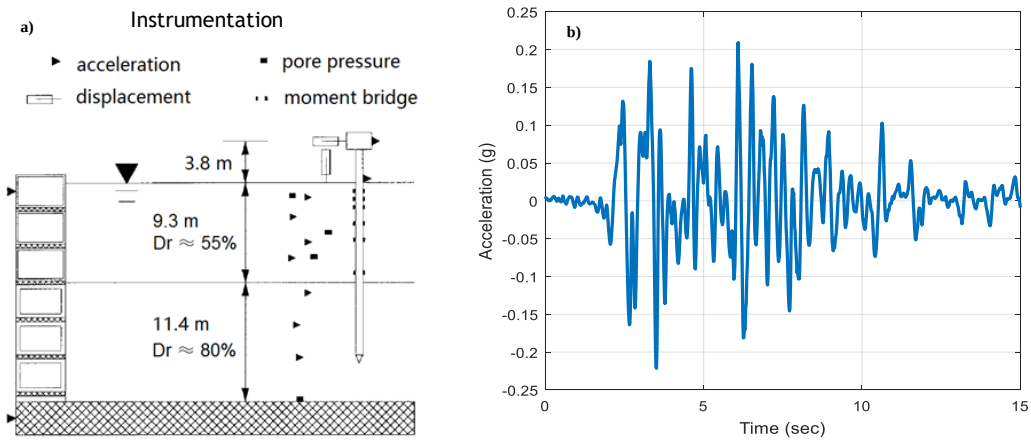

Figure 1: a) Partial model layout (Wilson 1998); and b) 1995 Kobe earthquake motion used in the centrifuge test and numerical modelling

Because of symmetry, only half of the model (32.0 m × 6.0 m × 20.7 m) was simulated as shown in Figure 2a. The horizontal black line in the soil represents the interface of the two soil layers. The saturated soil was modelled using 8-node BrickUP elements (element size varied) implemented with the PDMY02 material (Yang et al., 2003). The properties of the Nevada sand (Table 1) were derived from Choobbasti & Zahmatkesh (2016) and Karimi (2016). The bottom of the model was fixed in all three directions and nodes at the same depth on the left and right sides were tied together in the *x*-direction to simulate the free-field condition. For the front and back boundaries, translational displacements in the *y*-direction were not allowed. Moreover, water could drain from the ground surface only. Displacement-based beam elements were adopted to simulate the pile which was considered as an elastic material.

Based on Cheng & Jeremić (2009), a series of stiff elastic beam elements (rigid links) was used as "connections" between pile and soil nodes as illustrated in Figure 2b. Pile nodes and rigid link nodes were bonded in all six degrees of freedom (DOFs) (u_i and θ_i), and only the three translational DOFs (u_i) of the rigid link nodes were tied with soil nodes. These rigid links also prevent the soil opening from collapsing. For the nonlinear spring interface method, zero-length elements implemented with *p-y* and *t-z* spring materials were inserted between the rigid links and

the surrounding soil. Another zero-length element with *q-z* spring material was inserted between the pile toe node and the subjacent soil node. Due to liquefaction effects, the spring parameters were further modified by the coefficients of subgrade reaction from Boulanger et al. (2003).

The FE analyses were carried out in three loading stages: 1) self-weight loading, 2) pile installation loading and 3) seismic loading. The first stage was the consolidation process of the saturated level ground. During the second stage, a soil column at the model centre was excavated and the pile was then installed into the soil opening. A superstructure load was then added on the pile head followed by a static loading analysis. Finally, a seismic analysis was carried out by accelerating the model along the *x*-direction. There were also several seconds to rest the model after the loading.

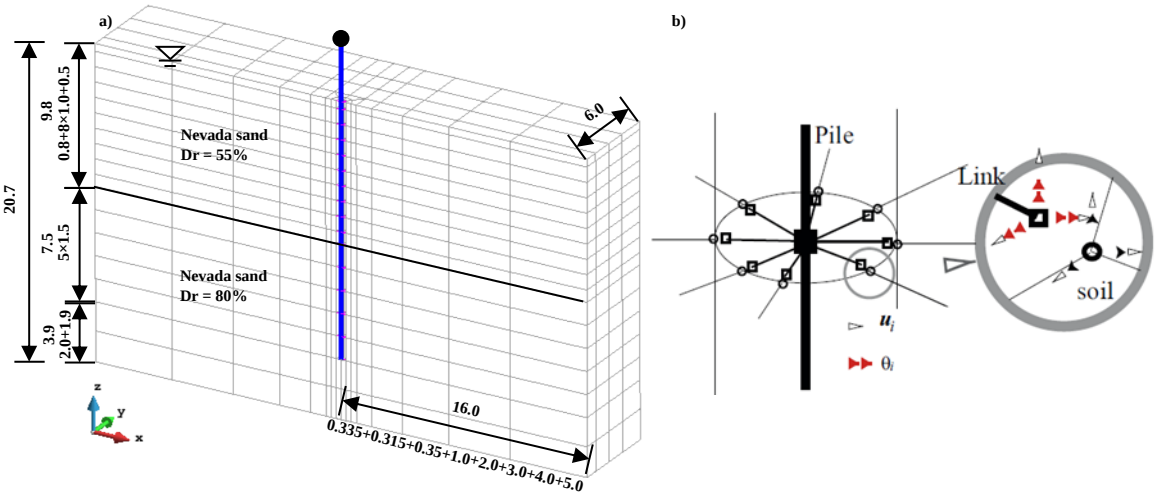

Figure 2: a) Model mesh; and b) Coupling of pile-soil nodes (Cheng & Jeremić 2009)

Table 1: Properties of Nevada sand used in the analysis

Model parameters	Nevada Sand	
Relative density D_r (%)	55	80
Reference effective confining pressure P_r' (kPa)	101	101
Reference shear modulus G_r (MPa)	63.0	88.4
Reference bulk modulus B_r (MPa)	168.2	236.0
Peak shear strain γ_{max}	0.1	0.1
Pressure dependency coefficient d	0.5	0.5
Friction angle φ_f (°)	33.5	36.5
Phase transformation angle φ_{PT} (°)	25.5	26.0
Contraction coefficients (c_1, c_2, c_3)	0.046, 3.42, 0.23	0.018, 1.48, 0.145
Dilation coefficients (d_1, d_2, d_3)	0.064, 3.0, 0.0	0.195, 3.0, 0.0
Number of yield surface	20	20
Liquefaction induced strain constants (liq_1, liq_2)	1.0, 0.0	1.0, 0.0
Void ratio e	0.685	0.618
Saturated unit weight ρ (ton/m^3)	1.98	2.03
Permeability coefficient k (m/s)	4.0×10^{-5}	2.5×10^{-5}

2.2 Verification of the numerical model

Figure 3 shows the comparison of the excess pore water pressure (EPWP) at the far-field between the numerical analysis (left and right boundaries of the model) and the centrifuge experiment at depths of 4.5 m and 7.0 m, which are approximately at the middle and bottom of the liquefiable layer, respectively. As results of numerical models with and without interface are the same, only one curve for the numerical model is plotted in the figure. The peak EPWP was well simulated at

depth of 4.5 m, but the simulation result has higher values at depth of 7.0 m. It is also evident that the simulation results showed the EPWP dissipated faster than that in the experiment. According to some researchers (e.g., Shahir et al., 2014), the permeability of the soil will increase during the liquefaction process and a variable permeability coefficient function should be adopted. This might be one of the reasons for the difference. However, the simulation does depict the accumulation process and the spikes well.

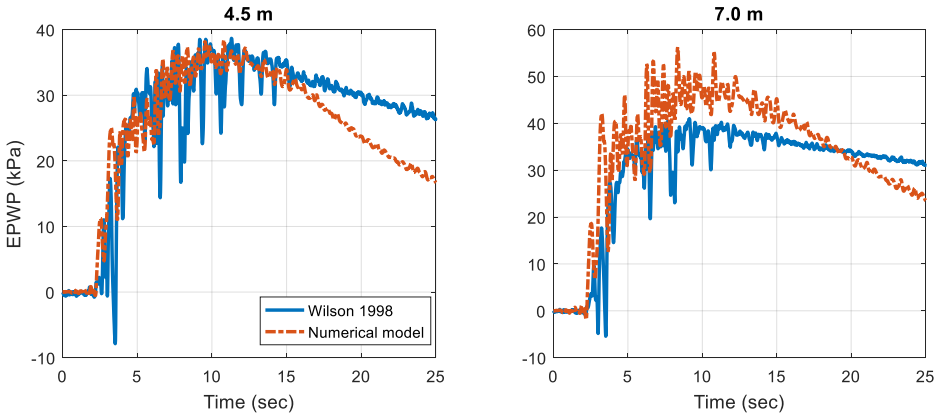

Figure 3: Free-field EPWP time history at different depths

The response of the pile at 2.0 m below the ground surface is shown in Figure 4 in which *p* and *y* represent the lateral reaction on the pile and the relative lateral displacement between the pile and soil, respectively. Good agreements can be detected between the experiment and simulation up to about 5 seconds after which the simulation response becomes smaller compared to the actual results. As shown in Figure 3, the increase in EPWP is found to be one of the reasons for this situation. This indicates that the adopted parameters or the performance of the PDMY02 material describing the liquefaction-induced deformation of the soil needs further enhancement. However, since the *p*-*y* relationship and the general trend of the response are satisfactory, this material was continued to be used in the next stage of the analysis.

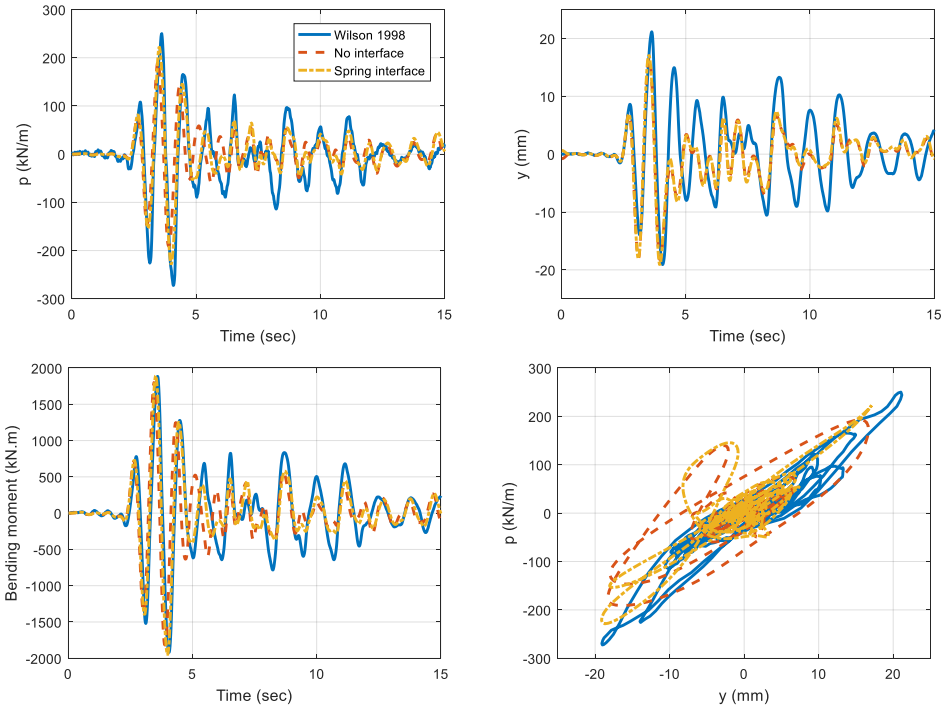

Figure 4: Dynamic response of vertical pile

Comparing the no-interface method with the spring interface method, one can observe that the difference between results is negligible. Neglecting the possible slippage or gapping on the soil-pile interface also seems to be the most common numerical approach emphasizing the soil-pile interaction problem (Zhang et al., 2017). Therefore, considering the advantages of simplicity and time-saving, the no-interface method was applied in the inclined pile analysis.

3 INCLINED PILE ANALYSIS

3.1 Model description

The same simulation method was applied in the inclined pile analysis, including the three-stage loading, coupling of pile-soil nodes and boundary conditions. Figure 5 depicts the meshing of the model and the inclined pile foundation with a raked angle θ = 10°. The model includes a soil block (36.0 m × 6.0 m × 15.0 m), two piles with the same inclination, a cap (3.0 m × 1.5 m × 1.0 m) and a column (4.0 m in length). The pile toe was 3.0 m above the model base and thicknesses of the liquefiable and non-liquefiable soil layers were 6.0 m and 9.0 m, respectively. In order to exclude the effects of soil-cap interaction, the cap was placed 1.0 m above the ground surface. A superstructure mass of 100 ton was added on top of the column. The diameter of the piles was set to 0.5 m for the sake of simplicity and the distance between the pile heads was 1.5 m (thrice the diameter). Material properties of the pile and Nevada sand were the same as the previous simulation. The cap and the column were elastic and had the same properties with the pile. By changing the raked angle (θ = 0°, 5°, 10°, 15° and 20°), a series of numerical simulations was conducted. It is worth mentioning that the 0° raked angle signifies that piles are vertical and the vertical length of piles is 13.0 m and independent from the raked angle.

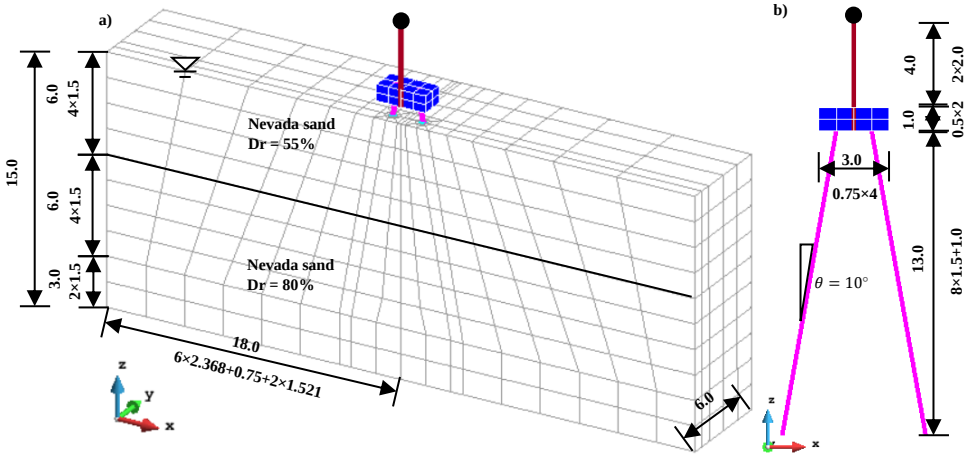

Figure 5: Inclined pile foundation model ($\theta = 10°$).

3.2 Comparison of results

The seismic response of the pile cap is shown in Figure 6a-d. With the increase of the inclination, the acceleration response of the cap (*Sa*) increases slightly at a period lower than 0.2 second (low period) and decreases at higher period as shown in Figure 6b. However, the horizontal displacement response of the pile is different with this investigation. As seen in Figure 6d, the response displacement *Sd* drops significantly as the inclination increase from 0° to 5° and then gradually decreases with the inclination. The reason may be that the inclined piles have enhanced the lateral resistance of the soil-pile-cap system. This indicates that the inclination of the pile may result in higher seismic acceleration or force on the cap but will be beneficial to reduce the lateral displacement. Similar conclusions can be obtained from the seismic response of the superstructure.

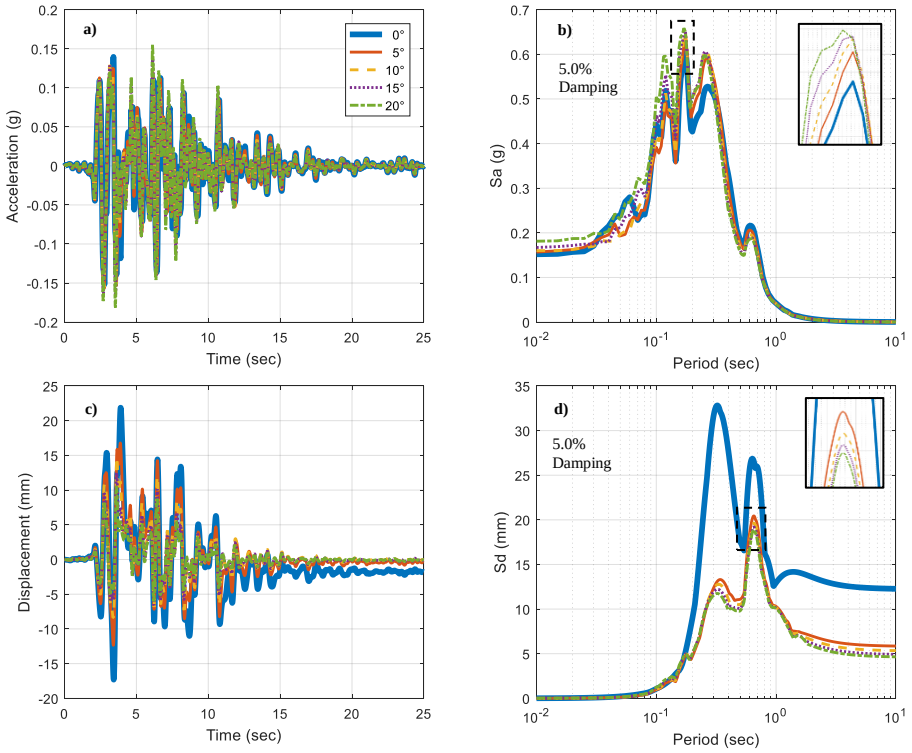

Figure 6: Seismic response of the cap

Figure 7a illustrates the EPWP development in the soil immediately adjacent to the pile at 3.0 m depth (the middle of the liquefiable layer). It is obvious that the pile inclination only results in slight fluctuations of the EPWP and has negligible effects on the developing process. Similar results can be obtained at other depths. Differences between the responses of the two piles are found to be ignorable which could be due to the fair symmetry of the input motion. Therefore, only results of the left pile are presented in the following figures. As demonstrated by Figure 7b, the inclination seems to reduce the maximum bending moment of the pile at around 3.0 m depth, the middle of the liquefiable layer; however, amplification can be observed near the pile head. With the increase of the inclination, a significant decrease in maximum positive axial force and increase of maximum shear force along the pile can be found in Figure 8. The presence of an initial shear force on inclined piles may be one of the reasons. As seen from Figure 9, piles with higher inclination angles suffer from higher soil resistance at the pile toe. Even though the inclination induces higher maximum pile displacement along most of the pile (below about 2.0 m), a reduction in the lateral displacement of the pile head can be observed.

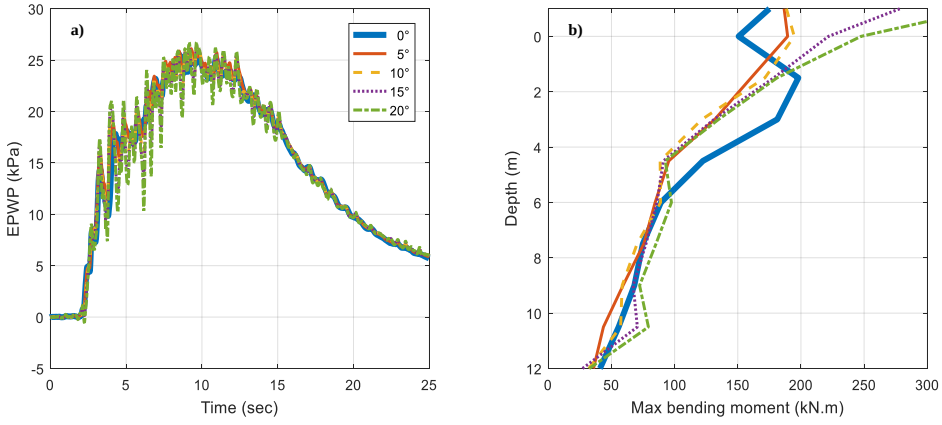

Figure 7: a) EPWP adjacent to the pile (3.0 m); and b) Max bending moment of the pile

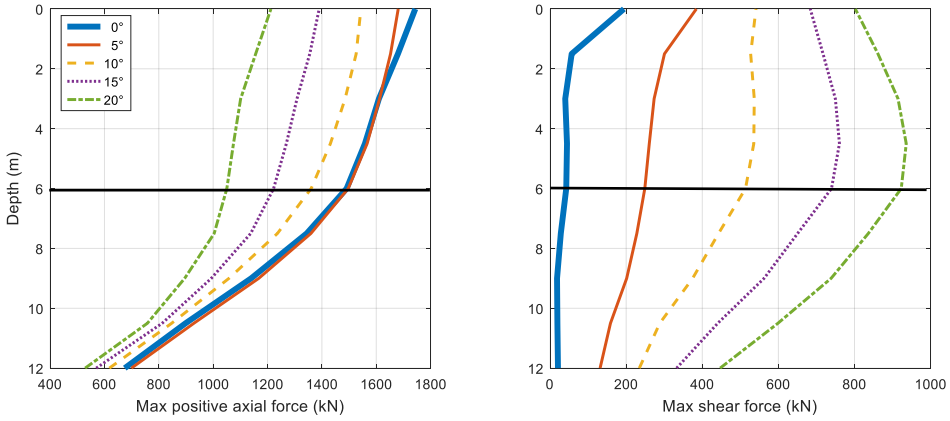

Figure 8: Max positive axial and shear force along the pile

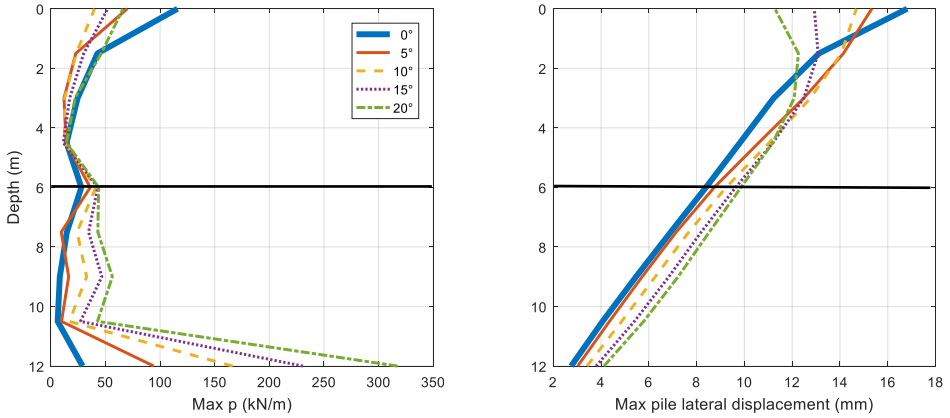

Figure 9: Max *p* and lateral displacement along the pile

4 CONCLUSIONS

To investigate the dynamic response of inclined piles in liquefiable soil, a comprehensive 3D FEM model has been developed using OpenSees. Spring interface method and no interface approach were compared with each other to detect the effects of soil-pile interaction. Results show that the difference between these two methods is negligible, at least for the model considered in this study. The influence of raked angles was then explored through the inclined pile analysis in which the no interface method was implemented. The pile inclination was found to be detrimental in inducing higher seismic force on the cap and superstructure and higher shear force along the pile. However, it played a beneficial role in reducing the lateral displacement of the above structures. Therefore, inclined piles are supposed to be designed with higher shear strength when used in the engineering practice. Otherwise, a combination of vertical and inclined piles with proper raked angle could be an alternative approach. This aspect may need further explorations for more details.

REFERENCES

Berrill, J. B. et al. (2001) Case study of lateral spreading forces on a piled foundation. *Géotechnique, 51*(6), 501–517.

Boulanger, R. W. et al. (2003) Pile foundations in liquefied and laterally spreading ground during earthquakes: centrifuge experiments & analyses. *Report No. UCD/CGM-03/01, Department of Civil and Environmental Engineering, UC Davis,*

205pp.

Cheng, Z., & Jeremić, B. (2009) Numerical modeling and simulation of pile in liquefiable soil. *Soil Dynamics and Earthquake Engineering*, *29*(11–12), 1405–1416.

Choobbasti, A. J., & Zahmatkesh, A. (2016) Computation of degradation factors of p-y curves in liquefiable soils for analysis of piles using three-dimensional finite-element model. *Soil Dynamics and Earthquake Engineering*, *89*, 61–74.

Dash, S. R., & Bhattacharya, S. (2015) Pore water pressure generation and dissipation near to pile and far-field in liquefiable soils. *International Journal of GEOMATE*, *9*(2), 1454–1459.

Gerolymos, N. et al. (2008) Evidence of beneficial role of inclined piles: Observations and summary of numerical analyses. *Bulletin of Earthquake Engineering*, *6*(4), 705–722.

Ghorbani, A. et al. (2014) Comprehensive three dimensional finite element analysis, parametric study and sensitivity analysis on the seismic performance of soil-micropile-superstructure interaction. *Soil Dynamics and Earthquake Engineering*, *58*, 21–36.

Goit, C. S., & Saitoh, M. (2013) Model tests and numerical analyses on horizontal impedance functions of inclined single piles embedded in cohesionless soil. *Earthquake Engineering and Engineering Vibration*, *12*(1), 143–154.

Karimi, Z. (2016) Seismic performance of shallow-founded structures on liquefiable ground An experimental and numerical study. *PhD Thesis*, University of Kurdistan.

Li, Z. et al. (2016) Centrifuge modeling of batter pile foundations under sinusoidal dynamic excitation. *Bulletin of Earthquake Engineering*, *14*(3), 673–697.

Mazzoni, S. et al. (2007) OpenSees command language manual. *Pacific Earthquake Engineering Research (PEER) Center*, 451.

McManus, K. et al. (2005) Inclined reinforcement to prevent soil liquefaction. In *Proceedings of the Annual NZSEE Technical Conference*, 523–533.

Shahir, H. et al (2014) Employing a variable permeability model in numerical simulation of saturated sand behavior under earthquake loading. *Computers and Geotechnics*, *55*, 211–223.

Subramanian, R. M., & Boominathan, A. (2016) Dynamic experimental studies on lateral behaviour of batter piles in soft clay. *International Journal of Geotechnical Engineering*, *10*(4), 317–327.

Wilson, D. W. (1998) Soil-pile-superstructure interaction in liquefying sand and soft clay. *PhD Thesis*, University of California, Davis.

Yang, Z. et al. (2003) Computational model for cyclic mobility and associated shear deformation. *Journal of Geotechnical and Geoenvironmental Engineering*, *129*(12), 1119–1127.

Zhang, L. et al. (2017) Seismic response of pile-raft-clay system subjected to a long-duration earthquake: centrifuge test and finite element analysis. *Soil Dynamics and Earthquake Engineering*, *92*, 488–502.